Green synthesis of ZnO nanoparticles using *Aphloia theiformis* leaf extract from Madagascar: Characterisations

Sambatra Rosa Ranaivoson [1, 2]
https://orcid.org/0000-0002-0999-8124
sambatrarosaranaivoson@ymail.com

Ravo Tokiniaina Ranaivoson [1]
https://orcid.org/0000-0003-2233-6106

Alain Gibaud [3]
https://orcid.org/0000-0002-7777-6427

Malik Maaza [4]
https://orcid.org/0000-0003-3429-509X

Raboanary Roland [2]
https://orcid.org/0000-0002-0819-2583

Abstract

We report a sustainable green synthesis of zinc oxide nanoparticles (ZnONPs) using an aqueous extract of *Aphloia theiformis*, an indigenous medicinal plant from Madagascar. The phytochemicals in the extract act as both reducing and stabilising agents. Zinc nitrate hexahydrate ($Zn(NO_3)_2.6H_2O$) was used as the precursor, and synthesis was carried out by a simple thermal process at 100 °C, followed by calcination at different temperatures to improve crystallinity. The nanoparticles were thoroughly characterised by SEM EDX, FTIR, XRD, Raman spectroscopy, and UV–Vis diffuse reflectance spectroscopy. The ZnONPs exhibit a quasi-spherical morphology with a relatively narrow size distribution (20–40 nm) and a pure hexagonal wurtzite phase, free of detectable secondary phases. The FTIR analysis confirms that polyphenols and flavonoids play a key role in the reduction and stabilisation of the nanoparticles. Raman spectroscopy reveals a dominant E_2(high) mode at 437 cm^{-1}, which is indicative of high crystallinity. Optical measurements show a band gap of 3.12–3.25 eV, consistent with semiconducting zinc oxide (ZnO). To the best of our knowledge,

1 National Institute of Nuclear Sciences and Techniques (INSTN-Madagascar).
2 Doctoral School of Physics and Applications, Faculty of Science, University of Antananarivo, Madagascar.
3 Institute of Molecules and Materials of Le Mans (IMMM), Le Mans University, France.
4 UNESCO-UNISA Africa Chair in Nanoscience-Nanotechnology, College of Graduate Studies, University of South Africa.

UNISA university of south africa PRESS
Nano-Horizons
Volume 5 | 2026 | #21942 | 17 pages
https://doi.org/10.25159/3005-2602/21942
ISSN 3005-2602 (Online)

this is the first report describing the use of *Aphloia theiformis* leaf extract for the green synthesis of ZnONPs. This study introduces *Aphloia theiformis* as a novel bioresource for the green synthesis of nanomaterials, opening new avenues for environmentally sustainable nanotechnology.

Keywords: nanoparticles; zinc oxide; green synthesis; *Aphloia Theiformis*; characterisation

1 Introduction

Zinc oxide nanoparticles (ZnONPs) are currently attracting growing interest owing to their optical, electronic, photocatalytic and antibacterial properties [1]. Zinc oxide (ZnO) is a Group II–VI semiconductor that crystallises in a wurtzite-type hexagonal structure. It has a wide direct band gap (~ 3.36 eV), strong ultraviolet absorption, high exciton binding energy (~ 60 meV), good chemical stability and low toxicity. These characteristics make it an attractive material for many applications, including optical detection, electronic devices, photocatalysis and antimicrobial materials [2], [3].

At the nanometric scale, the properties of ZnO are significantly enhanced by the quantum confinement effect, which modifies its optical and electronic response. Numerous studies have also indicated that ZnONPs exhibit significant antimicrobial activity against a wide range of pathogenic bacteria, justifying their use in the biomedical, food and environmental sectors [4], [5], [6]. Several physical and chemical methods can be used to synthesise ZnONPs, such as sol-gel, vapour deposition, thermal evaporation, microwave irradiation, laser deposition, and hydrothermal processes. However, most of these approaches require severe synthesis conditions (high temperatures, high pressures), expensive equipment and involve toxic solvents or reagents. They can have significant environmental impacts and limit their large-scale application [7], [8], [9].

In this context, so-called “green” synthesis methods appear to be a sustainable, simple and economical alternative. This approach is based on the use of reducing and stabilising agents of biological origin (microorganisms, enzymes, plant extracts). Among these, plant extracts are the most promising owing to their richness in secondary metabolites (polyphenols, flavonoids, tannins, alkaloids, proteins, polysaccharides) [10]. These biomolecules have the ability to reduce metal ions and stabilise the nanoparticles formed, while acting as capping agents, and therefore preventing particle agglomeration. Green synthesis also makes it possible to obtain nanoparticles that are more biocompatible, more stable and suitable for medical and environmental applications [11], [12].

Aphloia theiformis is a plant indigenous to Madagascar and is known for its antioxidant, antimicrobial, anti-inflammatory and photoprotective properties [13], [14]. Its high phenolic compound content and traditional uses suggest excellent potential as a source of biomolecules capable of reducing and stabilising metal nanoparticles or metal oxides

[15], [16]. Despite its pharmacological interest and documented bioactive properties, few studies have evaluated its effectiveness in the green synthesis of nanomaterials. To our knowledge, no previous study has been devoted to the use of aqueous extract from *Aphloia theiformis* leaves for the biosynthesis of ZnONPs.

Among medicinal plants, *Aphloia theiformis* has attracted increasing attention owing to its richness in polyphenols, flavonoids and xanthones, compounds known for their antioxidant and reducing properties. This plant is traditionally used for various therapeutic purposes and represents a promising natural source of bioactive molecules for green nanotechnology applications [17], [18]. Therefore, the use of *Aphloia theiformis* leaf extract in the present study is expected to facilitate the eco-friendly synthesis and stabilisation of ZnONPs while potentially enhancing their biological activity.

This study therefore aims to synthesise ZnONPs from an aqueous extract of *Aphloia theiformis* leaves and to characterise their structural, morphological and optical properties using advanced techniques (SEM-EDX, FTIR, XRD, Raman, photoreflectance). This approach contributes not only to the valorisation of a plant resource indigenous to Madagascar, but also to the development of environmentally friendly synthesis methods for nanomaterials with high application potential.

2 Materials and Methods

2.1 *Aphloia theiformis* (Ravimboafotsy) from Madagascar

Aphloia theiformis (Vahl) Benn., known locally as “Ravimboafotsy” belonging to the family Aphloiaceae, is an indigenous medicinal plant found in Madagascar, the Indian Ocean islands and other sub-Saharan African countries [17], [19], [20]. It grows as a shrub or small tree in humid forest regions and can reach several meters in height. The leaves are simple, alternate, and coriaceous with serrated margins. The flowers are small, whitish to yellowish in colour, and usually arranged in axillary inflorescences. Owing to its various therapeutic properties, this plant is widely used in traditional medicine for its anti-inflammatory, antipyretic, antimicrobial and antioxidant properties, and in cosmetics for its photoprotective and anti-ageing properties [13], [21]. Several studies have indicated that its leaves are particularly rich in phenolic compounds and flavonoids [14], [15].

The plant material was collected from the botanical garden named “Ferme de Morarano” in Ambatolampy, Antsirabe, Madagascar, in 2021. It was identified and authenticated based on its morphological characteristics by a botanist from SYGEDUR, at the Faculty of Science, University of Antananarivo, Madagascar, but no voucher specimen was deposited in a herbarium for this study.

2.2 Preparation of the Plant Extract

Fresh leaves of *Aphloia theiformis* were harvested, washed thoroughly with running water, then dried in the shade at approximately 25 °C. The dry leaves were ground to obtain a fine powder. To prepare the aqueous extract (Figure 1), 1 g of leaf powder was added to 50 mL of distilled water in an Erlenmeyer flask. The mixture was heated to 90 °C for 60 min on a hot plate. After cooling to room temperature, the solution was filtered using Whatman filter paper (2.5 µm) to remove plant residues. The clarified extract was stored at 4 °C until use.

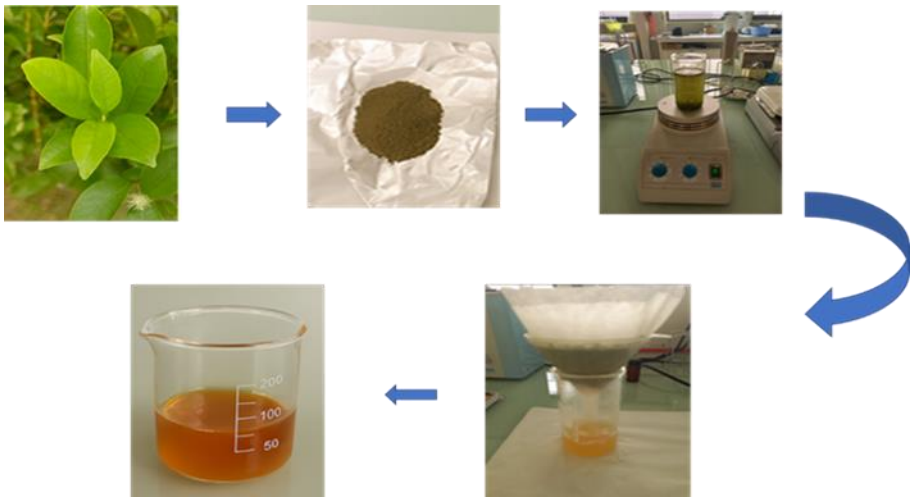

Figure 1: Preparation of the extract from the *Aphloia Theiformis* plant

2.3 Green Synthesis of ZnO Nanoparticles

The biosynthesis of ZnONPs was carried out according to the procedure illustrated in Figure 2. A total of 3.0 g of $Zn(NO_3)_2.6H_2O$ was dissolved in 100 mL of *Aphloia theiformis* extract. The mixture was kept at 100 °C under constant stirring (350 rpm) for 24 h, until the salt was completely dissolved and a white precipitate appeared, indicating the formation of nanoparticles. The pH of the reaction mixture was measured and maintained at approximately 10 during the synthesis process and all synthesis experiments were repeated at least three times to ensure reproducibility of the results.

Figure 2: Preparation of the solution and reduction to ZnONPs

The suspension obtained was distributed into small glass dishes and then dried in a Memmert UF30 oven at 100 °C for 2 h. The solid residues were then washed successively with distilled water and then ethanol to remove organic impurities.

After drying, the powders were calcined in a Nabertherm muffle furnace at 200, 300, 400 and 500 °C, each for 7 h, to improve crystallinity and remove residual biomolecules. The selected calcination temperatures (200–500 °C) were chosen to progressively remove organic residues from the plant extract and improve ZnO crystallinity without inducing structural degradation. The final ZnONPs powder was gently ground and stored for various analyses (Figure 3). The typical yield was approximately 0.45 g of ZnONPs per 1 g of ($Zn(NO_3)_2.6H_2O$) precursor.

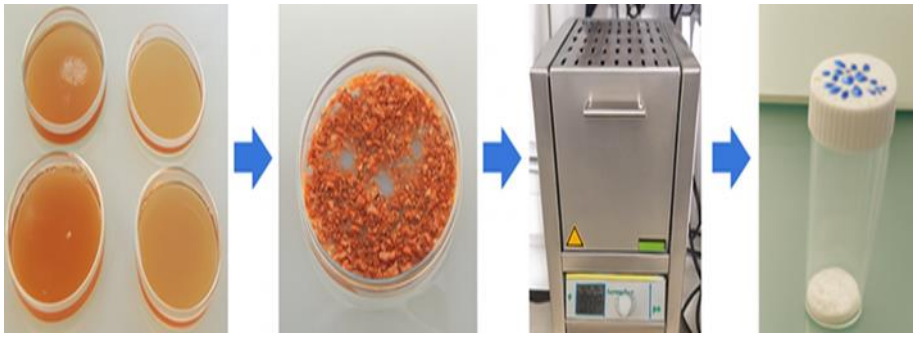

Figure 3: Purification of ZnONPs

2.4 Characterisation Techniques

The synthesised nanoparticles were characterised using the techniques described below.

X-Ray Diffraction (XRD)

The diffraction patterns were recorded on a PANalytical Empyrean diffractometer, using Cu Kα radiation (λ = 1.5406 Å), in a range from 10° to 90° (2θ) with a tube set at 40 kV and 40 mA. Peak indexing and structural refinement were performed using MAUD software, with reference to standard ZnO CIF files (wurtzite structure).

Scanning Electron Microscopy and EDX Analysis (SEM-EDX)

The morphology and size of the particles were studied using a ZEISS Gemini SEM 560 scanning electron microscope operating at 5 kV. The elemental composition was evaluated by energy dispersive X-ray spectroscopy (EDX).

Fourier Transform Infrared Spectroscopy (FTIR)

The FTIR spectra were recorded on a Bruker Vertex 70 spectrometer equipped with an ATR module in the range of 4 000–400 cm^{-1} at a resolution of 4 cm^{-1} with 32 scans. The data were processed with OPUS 7.5 and compared with the NIST Chemistry WebBook databases.

Raman Spectroscopy

Raman analyses were performed with a HORIBA Xplora spectrometer, using a 532 nm excitation laser. The laser power and acquisition times were adjusted to avoid thermal degradation of the material.

UV-Vis Diffuse Reflectance (Photoreflectance)

Photoreflectance measurements were performed using the Accent RPM 2000 system (KLA-Tencor), in quasi-normal reflection geometry, with a He–Ne laser (λ = 633 nm). The ZnONPs were deposited on a silicon substrate for optical gap analysis using the Tauc method.

3 Results and Discussion

3.1 Morphological Analysis and Elemental Composition (SEM-EDX)

The SEM micrographs reveal that the nanoparticles obtained are predominantly quasi-spherical in shape, with a few slightly hexagonal shapes. Their size, ranging from 20 to 40 nm, indicates a relatively homogeneous distribution. Moderate agglomeration is visible, a phenomenon typical of nanoparticles produced by green synthesis, due to the presence of residual biomolecules from the plant extract. This type of agglomeration has also been reported in the work of Buazar *et al*. [22] and Naiel *et al*. [23], where polyphenol-rich extracts play a dual role as reducing agents and stabilisers, while occasionally inducing slight interparticle interactions.

The EDX analysis confirms that the particles are mainly composed of zinc (Zn) and oxygen (O), with no significant traces of impurities, which attests to the good elemental purity of the ZnO produced. The measured proportions (Zn ≈ 43.32%; O ≈ 34.03%) are consistent with those reported in other green syntheses, notably those of Santhoshkumar *et al*. [24] and Aldeen *et al*. [25], which emphasise that plant-based approaches make it possible to obtain chemically clean nanoparticles without resorting to aggressive chemical agents. The agreement between SEM observations and EDX data confirms the effectiveness of *Aphloia theiformis* extract as a natural reducing and stabilising agent [23], [24].

Figure 4 shows an SEM micrograph and the associated EDX spectrum, illustrating the characteristic morphology and elemental composition of the synthesised ZnONPs. The SEM micrographs (Figure 4(a)) reveal that the synthesised material consists of dense, porous agglomerates of nanoparticles. Although individual particles require higher magnification to be fully resolved, they appear predominantly quasi-spherical in shape, with a few slightly hexagonal geometries, and with an estimated size ranging from 20 to 40 nm. This moderate agglomeration is a typical phenomenon of nanoparticles produced by green synthesis, due to the presence of residual biomolecules from the plant extract. This behaviour has also been reported by Buazar *et al*. [22] and Naiel *et al*. [23], where polyphenol-rich extracts play a dual role as reducing agents and stabilisers, while occasionally inducing slight interparticle interactions. The EDX analysis (Figures 4(c) and 4(d)) confirms that the particles are mainly composed of zinc (Zn ≈ 43.32 at.%.) and oxygen (O ≈ 34.03 at.%.).

The remaining carbon content (~ 22.65 at.%.) is attributed to both the carbon tape used during sample preparation and the residual organic capping agents from the plant. No other significant impurities were detected, attesting to the good elemental purity of the produced ZnO. The measured Zn/O proportions are consistent with those reported in other green syntheses, notably by Santhoshkumar *et al*. [24] and Aldeen *et al*. [25], which emphasise that plant-based approaches yield chemically clean nanoparticles without resorting to aggressive chemical agents. The agreement between SEM observations and EDX data confirms the effectiveness of *Aphloia theiformis* extract as a natural reducing and stabilising agent [23], [24].

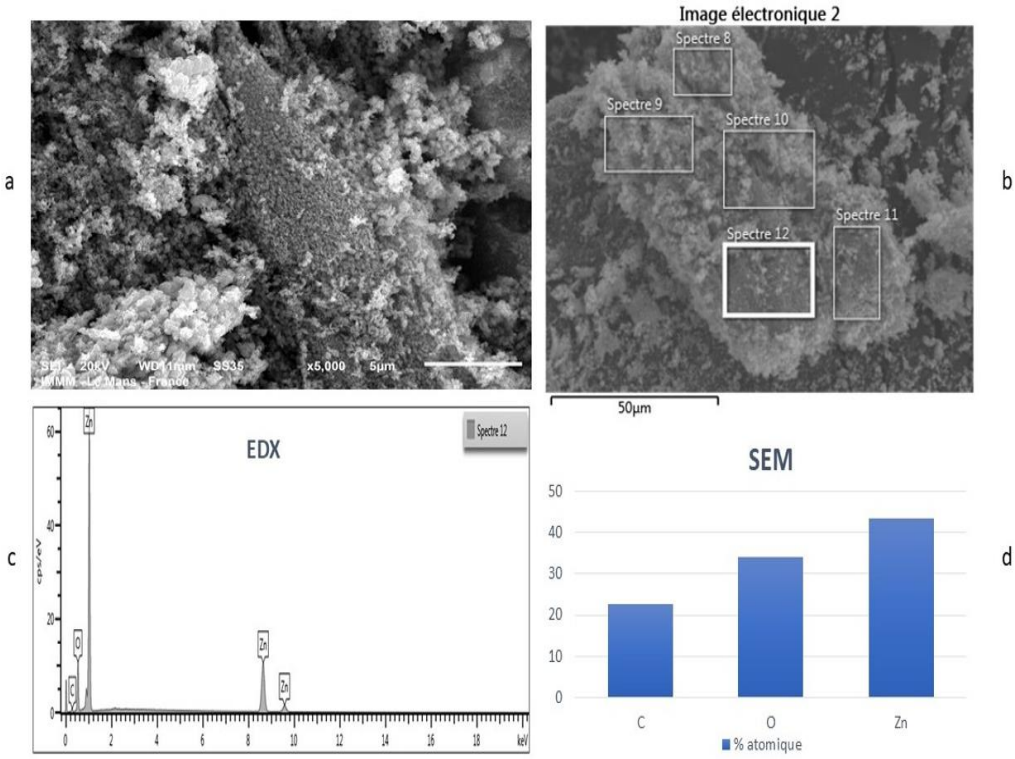

Figure 4: a) SEM micrograph of ZnONPs biosynthesised using *Aphloia theiformis* leaf extract; b) SEM image indicating the different selected regions used for elemental microanalysis (Spectra 8–12); c) EDX spectrum confirming the presence of Zn, O and C; d) atomic percentage distribution of the detected elements obtained from SEM–EDX analysis

3.2 Fourier Transform Infrared Spectroscopy Analysis

The FTIR spectra (Figure 5) highlight the functional groups derived from the biomolecules present in the *Aphloia theiformis* extract and involved in the reduction and subsequent stabilisation of the ZnONPs. The main bands observed are around 3 678 cm^{-1} (O–H of alcohols, phenols and carboxylic acids), 2 984 cm^{-1} (aliphatic C–H), 1 622 cm^{-1} (C = O of carbonyls and/or N–H of amides), 1 326–1 243 cm^{-1} (C–N and C–O), 1 061 cm^{-1} (C–O of polysaccharides and polyphenols) and 865 cm^{-1} (aromatic deformations = C–H). The presence of hydroxyl, carbonyl and phenolic functional groups confirms the involvement of phytochemicals such as flavonoids and polyphenols in the reduction of Zn2+ ions and stabilisation of the ZnONPs. These biomolecules adsorb on the nanoparticle surface, limiting excessive growth and agglomeration through capping effects. The gradual disappearance of organic bands

after calcination indicates decomposition of residual phytochemicals and improved purity of the ZnO crystalline phase.

All of these signals are characteristic of secondary metabolites such as polyphenols, flavonoids, tannins and proteins, which are known to play a key role in reducing metal ions and capping nanoparticles during green syntheses [9], [26]. These observations are consistent with the phytochemical composition of *Aphloia theiformis*, which is rich in phenolic compounds [13].

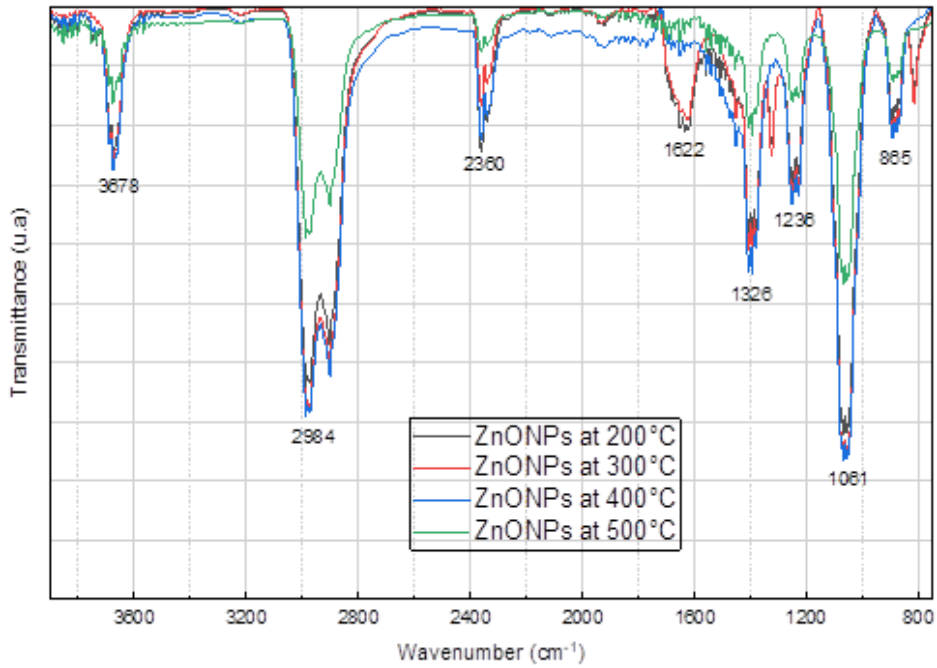

Figure 5: FTIR spectra of ZnONPs using *Aphloia theiformis* leaf extract after calcination at different temperatures, recorded in the range 4 000–400 cm^{-1} using ATR mode

The evolution of the spectra as a function of temperature shows a gradual decrease, then the virtual disappearance of the organic bands between 200 and 500 °C, reflecting the thermal degradation of the adsorbed biomolecules. This transformation, also reported in other green syntheses by Xiong *et al*. [27] and Naiel *et al*. [23], is accompanied by the appearance and strengthening of the characteristic Zn–O band located around 445 cm^{-1}, confirming the formation of a purer and better crystallised ZnO at high temperature [26], [27].

These results therefore demonstrate that the extract of *Aphloia theiformis* provides the functional groups necessary for the reduction and stabilisation of nanoparticles, while ensuring their gradual purification during calcination.

3.3 X-Ray Diffraction Analysis

The X-ray diffractogram (Figure 6) displays the characteristic peaks of the hexagonal wurtzite structure of ZnO, with reflections at 31.7°, 34.4°, 36.2°, 47.5°, 56.6°, 62.9°, 66.4°, 68.0° and 69.1°, assigned to the (100), (002), (101), (102), (110), (103), (200), (112) and (201) planes, respectively. These positions correspond closely to the JCPDS card 36 1451, confirming the formation of crystalline ZnO. The refinement performed using the MAUD software reveals no secondary phases, attesting to the structural purity of the nanoparticles.

The effect of calcination is clearly visible: at 200 °C, the broad, low intensity peaks indicate limited crystallinity, whereas at intermediate temperatures (300–400 °C) the peaks become sharper. At 500 °C they reach maximum intensity and reduced width, indicating improved structural organisation. This gradual improvement of crystallinity with temperature is typical behaviour for nanostructured ZnO, also reported for green, hydrothermal or sol gel syntheses [4], [26], [28], [29].

To quantify this evolution, the crystallite size was estimated from the most intense (101) peak using the Scherrer equation:

$$D = \frac{K\lambda}{\beta \cos\ \theta}$$

where $K = 0.9$ (shape factor), $\lambda = 0.15406$ nm (Cu Kα radiation), β is the integral breadth corrected for instrumental broadening, and θ is the Bragg angle. The measured full width at half maximum (FWHM) values and the resulting crystallite sizes D for each calcination temperature are presented in Table 1.

Table 1: Evolution of the full width at half maximum and crystallite size of ZnO as a function of calcination temperature, derived from the (101) peak located at 36.2° (Cu Kα)

Calcination temperature (°C)	FWHM of (101) peak (°)	Crystallite size *D* (nm)
200	0.85	10.2 ± 0.5
300	0.62	14.0 ± 0.6
400	0.48	18.1 ± 0.7
500	0.38	22.8 ± 0.8

The steady decrease in FWHM with temperature translates into an increase in crystallite size, from ~ 10 nm at 200 °C to ~ 23 nm at 500 °C. These values, on the order of a few tens of nanometres, are in good agreement with the dimensions observed by SEM, confirming homogeneous nanometric growth. Similar trends have been reported for ZnONPs synthesised from *Aloe vera* or *Elaeagnus angustifolia* extracts [6], [23].

In addition, Rietveld refinement yields lattice parameters a = 3.249 Å and c = 5.206 Å, in excellent agreement with the JCPDS 36–1451 reference (a = 3.249 Å, c = 5.206 Å). The agreement factors (R_{wp} < 10%, R_p < 8%) attest to the quality of the refinement and confirm the absence of significant lattice distortions.

The absence of parasitic peaks such as $Zn(OH)_2$ or metallic *Zn* demonstrates that *Aphloia theiformis* extract enables a single-phase *ZnO* to be obtained without the formation of crystalline intermediates. This structural purity, combined with crystallite sizes that can be controlled through temperature, is crucial for photocatalytic and optoelectronic applications, which is consistent with the conclusions of Naiel *et al*. [23] and Aldeen *et al*. [25].

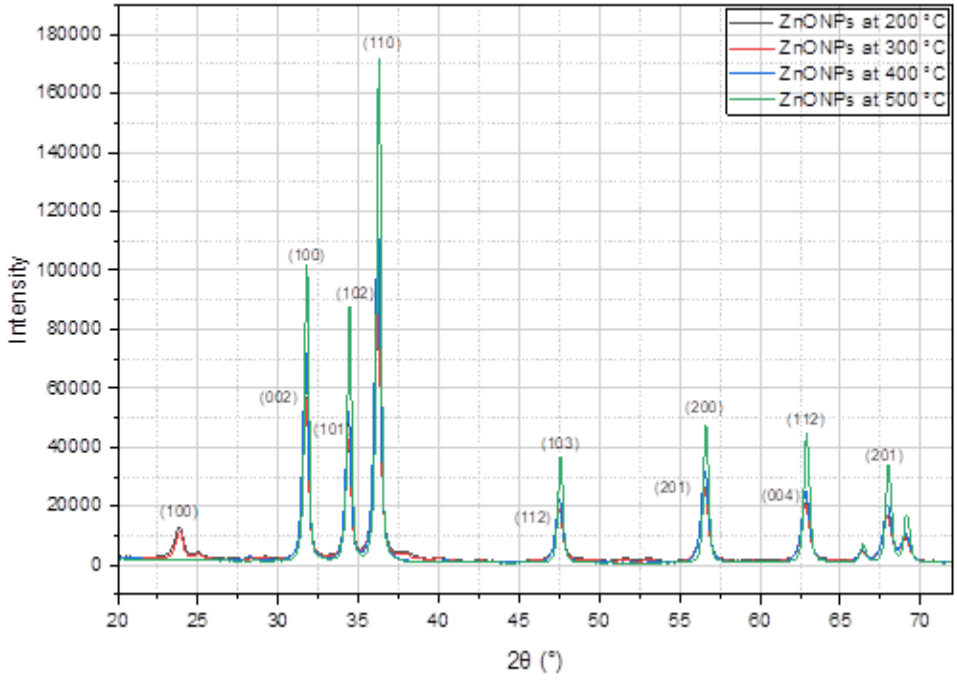

Figure 6: X-ray diffraction patterns of ZnONPs using *Aphloia theiformis* leaf extract after calcination at different temperatures

3.4 Raman Analysis

The Raman spectrum (Figure 7) shows an intense peak at 437 cm^{-1}, corresponding to the E_2(high) mode, which is the most characteristic vibrational signature of wurtzite-structured *ZnO*. This mode, generally associated with good crystallinity, is systematically reported for nanostructured *ZnO* [4], [27].

Secondary bands also appear around 330 cm^{-1} (multi-phonon mode E_2(high)–E_2(low)) and 380 cm^{-1} (mode A_1(TO)), in agreement with the vibrations expected in nanocrystalline *ZnO*. The presence of weak signals between 500 and 600 cm^{-1} indicates a low concentration of intrinsic defects, such as oxygen vacancies or zinc interstitials, frequently observed in *ZnO* synthesised at moderate temperatures. The weak Raman bands observed between 500 and 600 cm^{-1} may be associated with intrinsic structural defects such as oxygen vacancies and zinc interstitials, which are commonly reported in nanostructured ZnO synthesised under moderate thermal conditions.

The total absence of organic bands demonstrates the effectiveness of calcination at 500 °C, which allows the elimination of plant residues that served as reducing and stabilising agents. This observation is consistent with FTIR and XRD analyses, which also confirm the gradual purification of the material during the temperature increase [25], [26], [30].

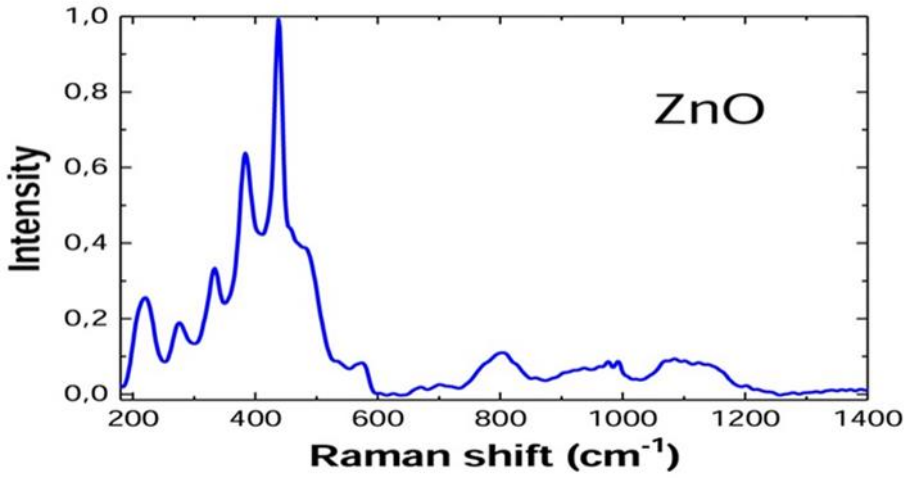

Figure 7: Raman spectrum of ZnONPs biosynthesised using *Aphloia theiformis* leaf extract after calcination showing the characteristic vibrational bands of ZnO

3.5 UV-Visible Diffuse Reflectance

The UV–Vis spectra (Figure 8) reveal strong absorption in the ultraviolet, with an edge located around 370 nm, which is characteristic of wide bandgap ZnO. Analysis of the

optical gap using the Tauc method, based on photoreflectance measurements, gives values between 3.12 and 3.25 eV, in agreement with those reported for green or hydrothermal synthesised ZnONPs [3], [4], [6], [23], [30].

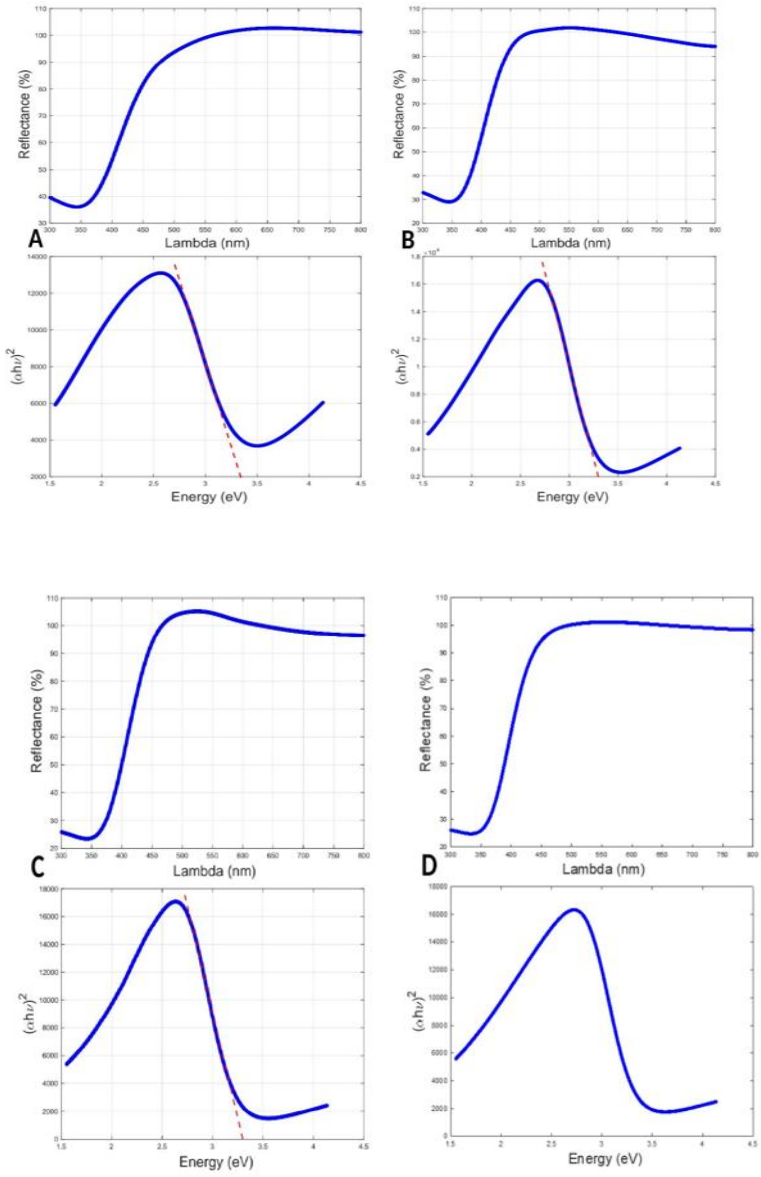

Figure 8: UV-Vis spectrum of ZnONPs using *Aphloia theiformis* leaf extract after calcination at different temperatures (A: ZnONPs at 200 °C, B: ZnONPs at 300 °C, C: ZnONPs at 400 °C, D: ZnONPs at 500 °C)

The evolution of the gap as a function of calcination temperature follows the well-known trend: higher calcination leads to an increase in crystallinity and a reduction in electronic defects (oxygen vacancies, Zn interstitials), resulting in a widening of the band gap [27], [29]. Conversely, samples calcined at lower temperatures exhibit a more pronounced absorption tail, reflecting structural disorder and a higher density of localised electronic states [26]. The slight variation in optical band gap values may be attributed to differences in crystallite size, defect concentration and degree of crystallinity induced by calcination temperature. Lower band gap values observed at lower temperatures could be associated with oxygen vacancies and localized defect states within the ZnO structure. These results confirm that green synthesis using *Aphloia theiformis* produces nanostructured ZnO with optical properties comparable to those reported in the literature, and is potentially suitable for photocatalytic and optoelectronic applications.

4 Conclusion

In this study, we successfully synthesised ZnONPs using a green synthesis approach that employs aqueous extract from *Aphloia theiformis* leaves as a natural reducing and stabilising agent. This method has the advantage of being simple, economical, non-toxic and compatible with the principles of sustainable chemistry.

Structural, morphological and optical analyses confirmed the formation of pure crystalline ZnO. The SEM images revealed quasi-spherical particles ranging in size from 20 to 40 nm, while EDX analysis showed an elemental composition dominated by zinc and oxygen, with no significant impurities. The FTIR spectra highlighted the role of biomolecules in the plant extract in the reduction and stabilisation of the NPs. The XRD and Raman results confirmed the hexagonal wurtzite structure of ZnO and improved crystallinity after calcination, particularly at 500 °C. Finally, photoreflectance analysis showed an optical gap between 3.12 and 3.25 eV, in line with the expected values for ZnO semiconductor.

Despite these promising results, certain limitations should be acknowledged. The natural variability of the plant extract composition can lead to batch-to-batch differences in nanoparticle size and morphology, and the specific biomolecules responsible for reduction and capping have not been isolated or identified. The as-synthesised nanoparticles show a tendency to agglomerate, which may affect their colloidal stability and functional performance in applications. The scalability of the synthesis process and the long-term stability of the ZnONPs also remain to be systematically evaluated.

The use of *Aphloia theiformis* as a natural source of bioactive metabolites is a promising alternative to conventional synthesis methods and paves the way for the commercialisation of this plant indigenous to Madagascar. The ZnONPs obtained have interesting properties for potential applications in photocatalysis, antimicrobial materials, environmental pollution control and optoelectronic devices. Future work could focus on an in-depth evaluation of the photocatalytic, antibacterial and

optoelectronic properties of the nanoparticles, as well as on optimising the synthesis conditions (pH, concentration, reaction time) to better control the size, morphology and colloidal stability of the ZnONPs. Identifying the key reducing and stabilising metabolites and comparing the extract with other indigenous Madagascan plants rich in phenolic metabolites would also provide valuable insights for further development.

5 References

[1] D. Sharma, S. Sharma, B. S. Kaith, J. Rajput and M. Kaur, "Synthesis of ZnO nanoparticles using surfactant free in-air and microwave method," *Appl. Surf. Sci*., vol. 257, no. 22, pp. 9661-9672, Sept. 2011, doi: 10.1016/j.apsusc.2011.06.094.

[2] Y. Zhang, *ZnO Nanostructures: Fabrication and Applications*. Royal Society of Chemistry, 2017. doi: 10.1039/9781788010238.

[3] A. Sirelkhatim *et al*., "Review on Zinc Oxide Nanoparticles: Antibacterial Activity and Toxicity Mechanism," *Nano-Micro Lett*., vol. 7, pp. 219–242, Jul. 2015, doi: 10.1007/s40820-015-0040-x.

[4] Z. L. Wang, "Zinc oxide nanostructures: growth, properties and applications," *J. Phys. Condens. Matter*, vol. 16, no. 25, pp. R829–R858, Jun. 2004, doi: 10.1088/0953-8984/16/25/R01.

[5] K. R. Raghupathi, R. T. Koodali and A. C. Manna, "Size-Dependent Bacterial Growth Inhibition and Mechanism of Antibacterial Activity of Zinc Oxide Nanoparticles," *Langmuir*, vol. 27, no. 7, pp. 4020–4028, Apr. 2011, doi: 10.1021/la104825u.

[6] A. Chaudhary, N. Kumar, R. Kumar and R. K. Salar, "Antimicrobial activity of zinc oxide nanoparticles synthesized from *Aloe vera* peel extract," *SN Appl. Sci*., vol. 1, p. 136, Jan. 2019, doi: 10.1007/s42452-018-0144-2.

[7] M. M. Oliveira, D. Ugarte, D. Zanchet and A. J. G. Zarbin, "Influence of synthetic parameters on the size, structure, and stability of dodecanethiol-stabilized silver nanoparticles," *J. Colloid Interface Sci*., vol. 292, no. 2, pp. 429–435, Dec. 2005, doi: 10.1016/j.jcis.2005.05.068.

[8] S. R. Senthilkumar and S. Thirumal, "Green tea (Camellia sinensis) mediated synthesis of zinc oxide (ZnO) nanoparticles and studies on their antimicrobial activities," *Int. J. Pharm. Pharm. Sci*., vol. 6, no. 6, pp. 461–465, Jan. 2014.

[9] V. K. Sharma, R. A. Yngard and Y. Lin, "Silver nanoparticles: Green synthesis and their antimicrobial activities," *Adv. Colloid Interface Sci*., vol. 145, no. 1–2, pp. 83–96, Jan. 2009, doi: 10.1016/j.cis.2008.09.002.

[10] J. Zivković *et al*., "Pharmacological properties of mangiferin: bioavailability, mechanisms of action and clinical perspectives," *Naunyn–Schmiedeberg's Arch. Pharmacol*., vol. 397, pp. 763–781, Feb. 2024, doi: 10.1007/s00210-023-02682-4.

[11] W. Huang, F. Tao, F. Li, M. Mortimer and L.-H. Guo, "Antibacterial nanomaterials for environmental and consumer product applications," *NanoImpact*, vol. 20, p. 100268, Oct. 2020, doi: 10.1016/j.impact.2020.100268.

[12] S. Zhang *et al*., "Green synthesis, biomedical effects, and future trends of Ag/ZnO bimetallic nanoparticles: An update," *Nanotechnol. Rev*., vol. 14, no. 1, Jan. 2025, doi: 10.1515/ntrev-2025-0186.

[13] M. C. N. Picot-Allain, "*Aphloia theiformis* (Vahl.) Benn.: A Plant with Various Therapeutic Properties," *J. Soil Plant Biol.*, vol. 2018, no. 1, pp. 16–20, Dec. 2018, https://pdfs.semanticscholar.org/e00f/b5e2d015f78b85305e2e295b30d03c759b2b.pdf.

[14] P. Danthu *et al*., "Biological Factors Influencing Production of Xanthones in *Aphloia theiformis*," *Chem. Biodivers*., vol. 7, no. 1, pp. 140–150, Jan. 2010, doi: 10.1002/cbdv.200900199.

[15] A. M. E. Shafey, "Green synthesis of metal and metal oxide nanoparticles from plant leaf extracts and their applications: A review," *Green Process. Synth*., vol. 9, no. 1, pp. 304–339, Jun. 2020, doi: 10.1515/gps-2020-0031.

[16] S. M. Amini, "Preparation of antimicrobial metallic nanoparticles with bioactive compounds," *Mater. Sci. Eng. C*, vol. 103, p. 109809, Oct. 2019, doi: 10.1016/j.msec.2019.109809.

[17] M. C. N. Picot and M. F. Mahomoodally, "Effects of *Aphloia theiformis* on key enzymes related to diabetes mellitus," *Pharm. Biol*., vol. 55, no. 1, pp. 864–872, Feb. 2017, doi: 10.1080/13880209.2016.1277765.

[18] D. Grauzdytė, A. Pukalskas, C. El Kalamouni and P. R. Venskutonis, "Mangiferin Rich Products from *Aphloia theiformis* (Vahl) Benn Leaves: Extraction, Fractionation, Phytochemical Characterization, and Antioxidant Properties," *Molecules*, vol. 25, no. 9, p. 2081, Apr. 2020, doi: 10.3390/molecules25092081.

[19] J.-P. Nicolas, *Plantes médicinales du Nord de Madagascar: Ethnobotanique antakarana et informations scientifiques*. Jardins du Mondes, 2023 https://www.ethnopharmacologia.org/prelude2020/pdf/biblio-hn-42-nicolas.pdf.

[20] M. Razafindraibe *et al*., "Medicinal plants used by women from Agnalazaha littoral forest (Southeastern Madagascar)," *J. Ethnobiol. Ethnomed.*, vol. 9, p. 73, Nov. 2013, doi: 10.1186/1746-4269-9-73.

[21] E. Clain *et al*., "Extract from *Aphloia theiformis*, an edible indigenous plant from Reunion Island, impairs Zika virus attachment to the host cell surface," *Sci. Rep*., vol. 8, p. 10856, Jul. 2018, doi: 10.1038/s41598-018-29183-2.

[22] F. Buazar, M. Bavi, F. Kroushawi, M. Halvani, A. Khaledi-Nasab and S. A. Hossieni, "Potato extract as reducing agent and stabiliser in a facile green one-step synthesis of ZnO nanoparticles," *J. Exp. Nanosci*., vol. 11, no. 3, pp. 175–184, May 2016, doi: 10.1080/17458080.2015.1039610.

[23] B. Naiel, M. Fawzy, M. W. A. Halmy and A. E. D. Mahmoud, "Green synthesis of zinc oxide nanoparticles using Sea Lavender (*Limonium pruinosum* L. Chaz.) extract: characterization, evaluation of anti-skin cancer, antimicrobial and antioxidant potentials," *Sci. Rep*., vol. 12, p. 20370, Nov. 2022, doi: 10.1038/s41598-022-24805-2.

[24] J. Santhoshkumar, S. V. Kumar and S. Rajeshkumar, "Synthesis of zinc oxide nanoparticles using plant leaf extract against urinary tract infection pathogen," *RET*, vol. 3, no. 4, pp. 459–465, Dec. 2017, doi: 10.1016/j.reffit.2017.05.001.

[25] T. S. Aldeen, H. E. A. Mohamed and M. Maaza, "ZnO nanoparticles prepared via a green synthesis approach: Physical properties, photocatalytic and antibacterial activity," *J. Phys. Chem. Solids*, vol. 160, p. 110313, Jan. 2022, doi: 10.1016/j.jpcs.2021.110313.

[26] M. Anbuvannan, M. Ramesh, G. Viruthagiri, N. Shanmugam and N. Kannadasan, "Synthesis, characterization and photocatalytic activity of ZnO nanoparticles prepared by biological method," *Spectrochim. Acta. A. Mol. Biomol. Spectrosc*., vol. 143, pp. 304–308, May 2015, doi: 10.1016/j.saa.2015.01.124.

[27] G. Xiong, U. Pal, J. G. Serrano, K. B. Ucer and R. T. Williams, "Photoluminesence and FTIR study of ZnO nanoparticles: the impurity and defect perspective," *Phys. Status Solidi C*, vol. 3, no. 10, pp. 3577–3581, Nov. 2006, doi: 10.1002/pssc.200672164.

[28] Y. Hu and H.-J. Chen, "Preparation and characterization of nanocrystalline ZnO particles from a hydrothermal process," *J. Nanopart. Res*., vol. 10, pp. 401–407, Mar. 2008, doi: 10.1007/s11051-007-9264-0.

[29] M. M. Almoneef *et al*., "Exploring the multi-faceted potential: Synthesized ZnO nanostructure – Characterization, photocatalysis, and crucial biomedical applications," *Heliyon*, vol. 10, no. 12, Jun. 2024, doi: 10.1016/j.heliyon.2024.e32714.

[30] J. Iqbal *et al*., "Green synthesis of zinc oxide nanoparticles using *Elaeagnus angustifolia* L. leaf extracts and their multiple in vitro biological applications," *Sci. Rep*., vol. 11, p. 20988, Oct. 2021, doi: 10.1038/s41598-021-99839-z.